

Design of PID Controller using LQR-Based Parameter Selection for DC Motor Position Control

Hartono¹, Eka Budiarto², Henry Nasution³

¹Mechatronics Engineering Department, Swiss German University, Jalur Sutera Barat No. 15, Tangerang 15143, Indonesia

²Information Technology Department, Swiss German University, Jalur Sutera Barat No. 15, Tangerang 15143, Indonesia

³Renewable Energy Engineering Technology, Bung Hatta University, Jl. Sumatera Ulak Karang Utara, Padang 25133, Indonesia

ARTICLE INFO

Article historys:

Received : 22/01/2025

Revised : 09/02/2025

Accepted : 18/02/2025

Keywords:

DC Motor; Linear Quadratic Regulator (LQR); Position Control; Proportional Integral Derivative (PID); Ziegler–Nichols

ABSTRACT

DC motors are widely applied in various fields due to their simple design, ease of control, and capability to generate high torque at low speeds. Position control of DC motors is crucial to ensure the performance and accuracy of the motorized electro-mechanical systems. The most common conventional control utilized in DC motors is the Proportional Integral Derivative (PID) controller. In this paper, the Linear Quadratic Regulator (LQR) approach is used to determine PID controller parameters for DC motors. The LQR approach, based on optimal control theory, offers a systematic alternative to traditional methods for tuning PID controllers. The results show that the designed controllers outperform the Ziegler–Nichols tuned PID, with the recommended controller Ctrl 1, achieves a settling time of 1.2953 s, an overshoot of 0.5%, and a steady-state error of 0.0043.



This work is licensed under a [Creative Commons Attribution 4.0 International License](https://creativecommons.org/licenses/by/4.0/)

Corresponding Author:

Hartono

Mechatronics Engineering Department, Swiss German University, Jalur Sutera Barat No. 15, Tangerang 15143, Indonesia

Email: har.tono@sgu.ac.id

1. INTRODUCTION

DC motors are electric motors that provide high starting torque and precise speed control by converting direct current electrical energy to mechanical energy [1–3]. Due to their simple design, ease of control, and capability to produce high torque at low speeds, DC motors are widely utilized in a variety of applications, including industrial automation, robotics, automotive, agriculture, and home appliances [4–7]. Since these motors are the main actuator component of the system, the appropriate controller should be designed to these motors to achieve good performance, precise speed and position, and efficient energy usage.

There are numerous studies related to speed and position control for DC motors. The most popular control technique is the PID controller, with its simplicity, intuitive design, good performance in linear systems, and capability for real-time adjustment [8]. PID parameters can be decided by several techniques, such as classical methods like manual tuning [9], Ziegler–Nichols, and Cohen–Coon that use reaction curves or ultimate gain [10] and optimization methods by minimizing error for better performance [11]. Additionally, frequency domain approaches ensure robustness, while modern techniques, including trial-and-error, genetic algorithms, and fuzzy logic, adapt to complex systems [12]. The other techniques are machine learning methods [13], Model Predictive Control (MPC) [14], and software tools like auto-tuners to provide convenient automated tuning solutions [15].

In this study, PID parameters will be selected using Linear Quadratic Regulator (LQR) approach, that offers a systematic framework for optimizing control gains. The LQR method is based on optimal control theory and offers a reliable alternative to the trial-and-error tuning methods often used in PID control design. By formulating the PID controller as a three-term structure compatible with the quadratic cost function of the LQR. This theory was first introduced in 1971 by Williamson and Moore [16].

2. RESEARCH METHOD

This research began with a literature study on DC motors and their control methods. It proceeded with mathematical modeling, followed by the design of the controllers. Simulations were then conducted using software to evaluate the performance of the designed controllers compared to Ziegler–Nichols method and analyze which controller is suitable for the system requirement.

2.1. Mathematical Model

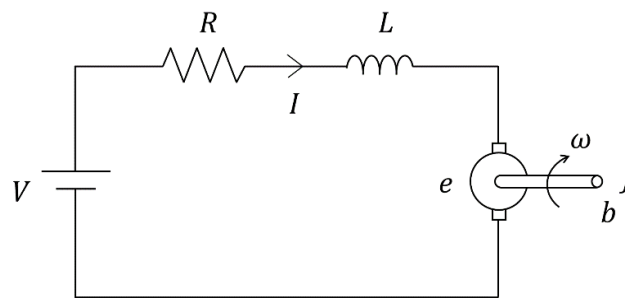


Figure 1. Equivalent circuit of a DC motor

DC motor is an actuator that uses the magnetic field force between the induced magnet from the winding, which is powered by an electric current flowing through the rotor, and the permanent magnet on the stator to transform electrical energy into mechanical energy [17]. Figure 1 illustrates a DC motor's equivalent circuit. The armature circuit's voltage equation can be expressed as the following equation using Kirchhoff's voltage law.

$$V = IR + L \frac{dI}{dt} + e \quad (1)$$

Where V is the voltage supply of DC motor, I is electric current, L is the inductance of the winding, R is resistance, and e is back electromotive force voltage, which is the product of the angular velocity ω and a constant k_e . Then, the electric circuit equation can be rewritten as equation (2).

$$\frac{dI}{dt} = -\frac{k_e}{L} \dot{\theta} - \frac{R}{L} I + \frac{1}{L} V \quad (2)$$

Meanwhile, the mechanical equation of the DC motor can be written as follows.

$$\tau = J\alpha + b\omega \quad (3)$$

With τ as the induced torque, J as the moment of inertia, α as the angular acceleration, b as the friction coefficient, and ω as the angular velocity. The induced torque is the product of the torque constant k_τ and the electric current I flowing through the rotor windings. Therefore, the mechanical equation can be expressed as:

$$\begin{aligned} k_\tau I &= J\ddot{\theta} + b\dot{\theta} \\ \frac{d\dot{\theta}}{dt} &= -\frac{b}{J}\dot{\theta} + \frac{k_\tau}{J} I \end{aligned} \quad (4)$$

Based on equation (2) and (4), by defining the state variables $x_1 = \theta$, $x_2 = \dot{\theta}$, $x_3 = I$, and $u = V$, the system's state space can be written as:

$$\begin{bmatrix} \dot{x}_1 \\ \dot{x}_2 \\ \dot{x}_3 \end{bmatrix} = \begin{bmatrix} 0 & 1 & 0 \\ 0 & -\frac{b}{J} & \frac{k_\tau}{J} \\ 0 & -\frac{k_e}{L} & -\frac{R}{L} \end{bmatrix} \begin{bmatrix} x_1 \\ x_2 \\ x_3 \end{bmatrix} + \begin{bmatrix} 0 \\ 0 \\ \frac{1}{L} \end{bmatrix} u \quad (5)$$

$$y = [1 \quad 0 \quad 0] \begin{bmatrix} x_1 \\ x_2 \\ x_3 \end{bmatrix} \quad (6)$$

Table 1. Physical parameters of DC motor used in this study

Parameter	Value
Friction coefficient, b	0.00105 Nms
Moment of inertia, J	0.0054 kg m ²
Torque constant, k_τ	0.507 Nm/A
Back emf constant, k_e	0.507 V/rad/s
Inductance, L	0.0125 H
Resistance, R	7.102 Ω

The physical parameters of the DC motor used in this study are shown in Table 1. Then, by substituting those physical parameters, the state space matrixes are obtained.

$$A = \begin{bmatrix} 0 & 1 & 0 \\ 0 & -0.19 & 93.89 \\ 0 & -40.56 & -568.16 \end{bmatrix} \quad B = \begin{bmatrix} 0 \\ 0 \\ 80 \end{bmatrix} \quad C = [1 \quad 0 \quad 0] \quad D = 0$$

2.2. Controller Design

Before designing the controller, the controllability of the system is analyzed to determine whether the system is controllable. If the system is able to change from one state to another in a limited amount of time, it is said to be controllable [18]. The controllability matrix M can be expressed as follows.

$$M = [B \quad : \quad AB \quad : \quad A^2B]$$

$$M = \begin{bmatrix} 0 & 1 & 7511.11 \\ 0 & 7511.11 & -4.27 \times 10^6 \\ 80 & -40.56 & 2.55 \times 10^7 \end{bmatrix}$$

The rank of the matrix was calculated as 3, matching with the system's dimension ($n = 3$). This indicates that the controllability matrix is full rank, and the system is fully controllable. Furthermore, in this article the controller to be designed is an LQR-tuned PID, which is a PID control with LQR as the parameter's selector for PID gain values K_p , K_i , and K_d .

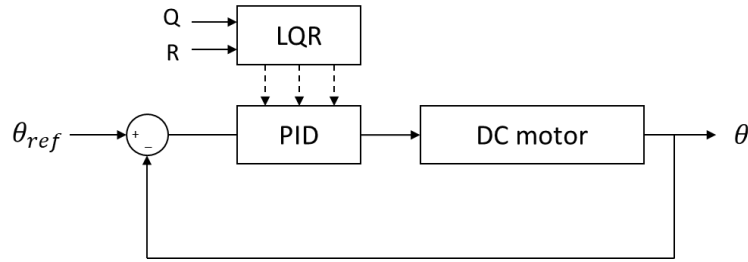


Figure 2. Block diagram of designed DC motor position control

The block diagram of the designed system to control the position of a DC motor is shown in Figure 2. Mathematical model of DC motor from equation (5) and (6) can be rewritten as follows:

$$\begin{aligned} \dot{x} &= Ax + Bu & x(t_0) &= 0 \\ y &= Cx \end{aligned} \quad (7)$$

x is the solution of equation (7), u is assumed as the output from the PID controller with input y , so that the output can be expressed as the equation (8).

$$u = K_1 \int_0^t y dt + K_2 y + K_3 \dot{y} \quad (8)$$

with K_1 , K_2 , and K_3 are PID gains.

$$K_1 = \frac{K_p}{T_i}; \quad K_2 = K_p; \quad K_3 = K_p T_d$$

Where K_p is proportional gain, T_i represents time integral, and T_d denotes time derivative from PID controller. Then, control law (8) is stated as state feedback control by using equation (7). From those equations, it can be obtained:

$$\begin{aligned} y &= Cx \\ \dot{y} &= CAx + CBu \\ \ddot{y} &= CA^2x + CABu + CB\dot{u} \end{aligned} \quad (9)$$

by applying the equation (9) to equation (8), result in:

$$\begin{aligned} \dot{u} &= K_1 y + K_2 \dot{y} + K_3 \ddot{y} \\ (1 - K_3 CB)\dot{u} &= (K_3 CA^2 + K_2 CA + K_1 C)x + (K_3 CAB + K_2 CB)u \end{aligned} \quad (10)$$

The notation \hat{K} is used to denote the normalized value of K .

$$\hat{K}^T = \begin{bmatrix} \hat{K}_1 \\ \hat{K}_2 \\ \hat{K}_3 \end{bmatrix} = (1 - K_3 CB)^{-1} \begin{bmatrix} K_1 \\ K_2 \\ K_3 \end{bmatrix} \quad (11)$$

$$\dot{u} = \hat{K}^T \begin{bmatrix} C^T \\ A^T C^T \\ (A^2)^T C^T \end{bmatrix} x + \hat{K}^T \begin{bmatrix} 0 \\ B^T C^T \\ B^T A^T C^T \end{bmatrix} u \quad (12)$$

The equation (12) can be simplified as:

$$u_a = K_a x_a \quad (13)$$

with

$$u_a = \dot{u}, \quad x_a = [x \quad u]^T$$

$$K_a = \begin{bmatrix} C^T & A^T C^T & (A^2)^T C^T \\ 0 & B^T C^T & B^T A^T C^T \end{bmatrix} \hat{K} = \Gamma \hat{K} \quad (14)$$

the augmented system equation based on equations (7) and (14) is as follows.

$$\dot{x}_a = A_a x_a + B_a u_a \quad (15)$$

$$A_a = \begin{bmatrix} A & B \\ 0 & 0 \end{bmatrix}; \quad B_a = \begin{bmatrix} 0 \\ 1 \end{bmatrix} \quad (16)$$

By solving the Riccati equation (17), \hat{K} can be determined, and the values of K_1 , K_2 , and K_3 can be calculated. In other words, the gains for PID control can be obtained.

$$A_a^T P + P A_a - P B_a R^{-1} B_a^T P + Q = 0 \quad (17)$$

$$\hat{K}^T = -R^{-1} B_a^T P \quad (18)$$

3. RESULTS AND DISCUSSION

To verify the feasibility of the designed controller, simulations were conducted by using the software. In these simulations, the matrices Q and R are chosen for the LQR parameters. Where Q represents the weighting matrix for the state variables, influencing how deviations from desired states affect the control effort. Matrix R , on the other hand, specifies the weighting on control inputs, influencing how much control effort is penalized relative to the state deviations.

$$Q = \begin{bmatrix} q_1 & 0 & 0 & 0 \\ 0 & q_2 & 0 & 0 \\ 0 & 0 & q_3 & 0 \\ 0 & 0 & 0 & q_4 \end{bmatrix} \quad R = 1$$

The fixed value for parameter R is chosen, while parameter Q is varied by changing the values of elements q_1 , q_2 , q_3 , and q_4 . The elements of matrix Q are selected through the empirical approach of trial and observation. Initially, random values were set to test how they affected the system. The values are then improved in steps where each step response is compared, and the aim is to reach a reasonable trade-off between system stability, response speed, and the amount of control effort needed. While this approach does not rely on a systematic optimization method, it does provide a means of practical tuning according to how the system performs. With these variations in the LQR parameters, different PID gains and step responses of the system are obtained, as shown in the following Table 2 and Table 3 respectively.

Table 2. LQR parameters and PID gains

Controller	LQR parameter					PID Gain		
	q_1	q_2	q_3	q_4	R	K_p	K_i	K_d
Ctrl 1	0.0001	15	1	5	1	1.0514	0.0100	0.0019
Ctrl 2	0.001	10	2	4	1	0.7640	0.0316	0.0014
Ctrl 3	0.01	5	3	3	1	0.4405	0.1000	0.0008
Ctrl 4	0.1	20	2	2	1	1.3686	0.3162	0.0024
Ctrl 5	1	25	2	6	1	1.6644	1.0000	0.0030

The relationship between the corresponding PID gains and the LQR parameters (Q and R) is shown in Table 2. The diagonal elements of state cost matrix Q (q_1 , q_2 , q_3 , q_4) affect the weight given to state variables in the optimization process, while the control input cost matrix R , is kept constant at $R=1$ to maintain consistent penalty on control effort. These LQR parameters are used to tune the PID gains (K_p ,

K_i , K_d), where K_p adjusts the system's response to current errors, K_i addresses accumulated errors to eliminate steady-state error, and K_d mitigates future errors to reduce overshoot.

As q_1 and other elements of Q increase, the PID gains show a corresponding adjustment to achieve the desired control performance. Lower q_1 values (e.g., Ctrl 1) result in more conservative gains, while higher q_1 values (e.g., Ctrl 5) lead to higher gains, figuring responsiveness and control effort. This trend reflects a systematic method to tune the balance between system responsiveness, stability, and control effort, offering flexibility in designing controllers for various applications, from conservative to aggressive control strategies. Furthermore, the effect of other elements of Q must also be considered. The value of q_2 primarily influences the integral gain K_i , which affects steady-state performance. A higher q_2 tends to result in a higher K_i , improving steady-state accuracy but also increasing the risk of oscillations. The elements q_3 and q_4 impact the derivative gain K_d , which affects the damping characteristics of the system. Lower values of q_3 and q_4 may lead to a lower K_d , potentially reducing overshoot but also slowing down the response. On the other hand, higher values of q_3 and q_4 contribute to increased K_d , improving damping but possibly require higher control effort. The step responses of the designed controllers, compared with Ziegler–Nichols (ZN) tuned PID with gain $K_p = 175.8$, $K_i = 3516$, and $K_d = 2.1975$ are displayed in Figure 3.

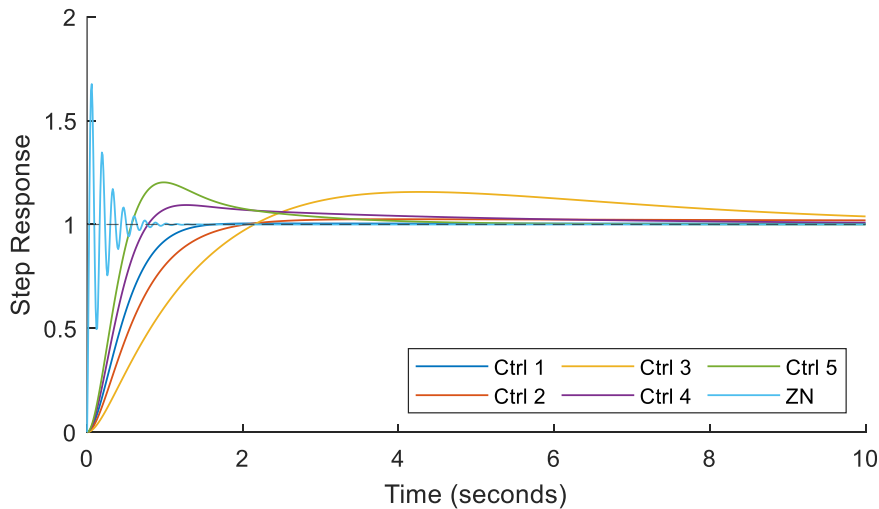


Figure 3. Step responses of designed controllers and ZN-tuned PID

Table 3. Comparison of step responses for different controllers

Controller	Step response performance			
	Rise Time (s)	Settling Time (s)	Overshoot (%)	Steady-State Error
Ctrl 1	0.7947	1.2953	0.50	0.0043
Ctrl 2	1.1133	9.9806	2.53	0.0200
Ctrl 3	1.5050	11.8510	15.66	0.0388
Ctrl 4	0.5219	6.8382	9.36	0.0089
Ctrl 5	0.3930	3.7631	20.27	0.0002
ZN	0.0197	0.6898	68.21	3.33×10^{-16}

For DC motor position control, choosing the proper controller is crucial, depending on the specific performance requirements of the application, including response speed, stability, and precision. Based on the step response data shown in Table 3, it can be seen that Ctrl 1 stands out with a balanced performance, featuring a moderate rise time of 0.7947 seconds and a settling time of 1.2953 seconds, with minimal overshoot at 0.50% and a very small steady-state error of 0.0043. This makes it a good option for applications where precision and stability are important. In other side, Ctrl 5 achieves the

fastest rise time of 0.3930 seconds and a settling time of 3.7631 seconds, with an impressive steady-state error of 0.0002, however it comes with a significant overshoot of 20.27%. This indicates that Ctrl 5 is more suitable for the system where a quick response is necessary, and the overshoot can be accepted. Meanwhile, Ctrl 4 strikes a balance with a relatively quick rise time of 0.5219 seconds, moderate overshoot of 9.36%, and a low steady-state error of 0.0089, making it suitable for applications that need a compromise between speed and precision.

The other controllers, Ctrl 2 and Ctrl 3, show longer settling times, greater overshoot, and higher steady-state errors, making them less suitable for precise position control tasks. In the other hand, ZN-tuned PID controller provides the best response time with a very small steady-state error of 3.33×10^{-6} which is almost zero, but with very high overshoot of 68.21%. This excessive overshoot makes the ZN-tuned PID unsuitable for motor position control in this case. In summary, Ctrl 1 is recommended for applications that prioritize stability and accuracy, while is preferable for those emphasizing speed.

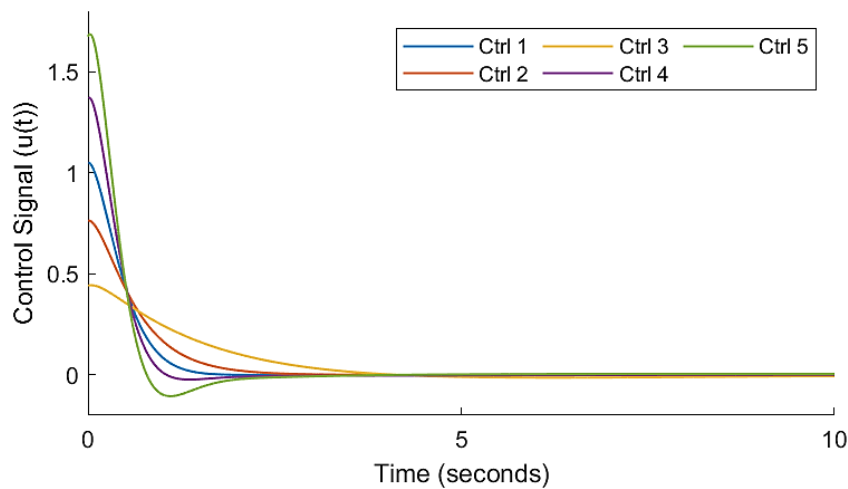


Figure 4. Control signal of designed controllers

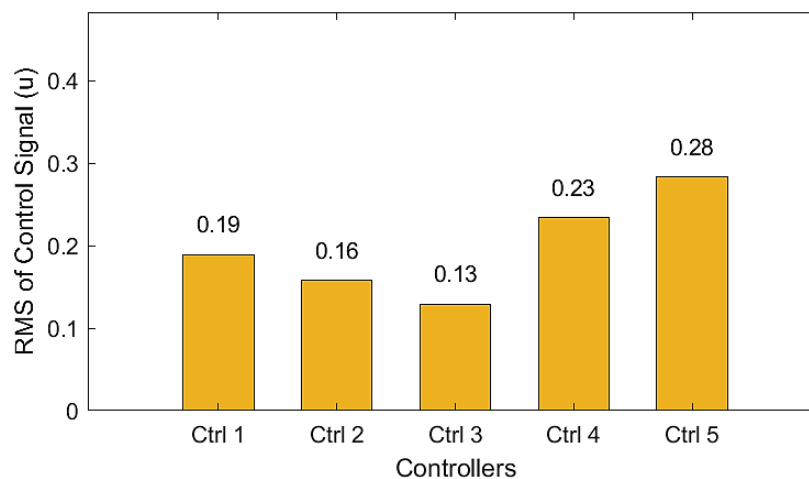


Figure 5. RMS of control signal

Additionally, the root mean square (RMS) values of control signal are shown in Figure 5, illustrating the value that is proportional with the energy required by each controller. Lower RMS values indicate less energy consumption, with Ctrl 3 being the most energy-efficient while Ctrl 5 consuming the highest energy. This highlights the trade-off between energy efficiency and performance, as more responsive controllers like Ctrl 5 tend to require greater control effort. For applications emphasizing energy savings, controllers like Ctrl 3 are more suitable, while high-performance tasks may justify higher energy consumption. Based on the step responses and control signal graphs, Ctrl 1 is chosen for DC motor position control due to its good response and moderate energy consumption compared to

another designed controllers. Furthermore, the ZN-tuned PID controller is not chosen for this system due to its high control signal magnitude, with the RMS value of 22.49, indicating excessive energy consumption. The control signal of the ZN-tuned PID controller is shown in Figure 6.

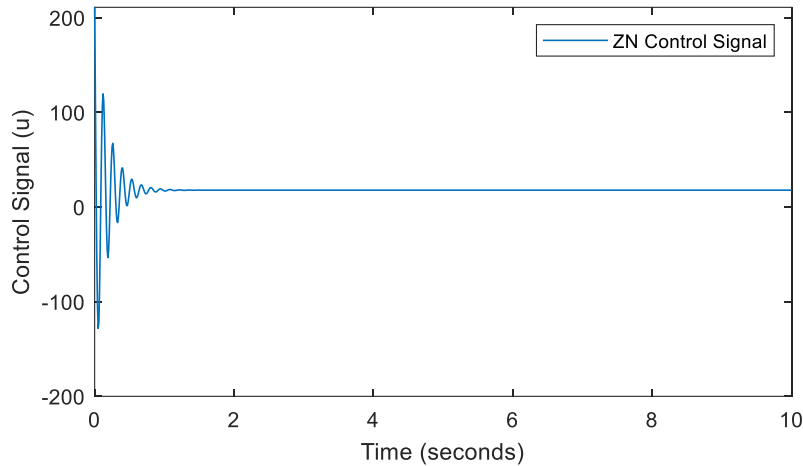


Figure 6. Control signal of ZN-tuned PID controller

4. CONCLUSION

This study demonstrates the effective tuning of PID controller gains using LQR parameters by varying the state weighting matrix Q while keeping R constant. The diagonal elements of Q significantly influence PID gains, shaping the system's response. Step response analysis highlights the controller's suitability for various applications. Ctrl 1 delivers balanced performance with minimal overshoot, short settling time, and negligible steady-state errors, ideal for precision tasks. Ctrl 5 provides the fastest response with very low steady-state error but high overshoot, suitable for speed-prioritized tasks. Ctrl 4 strikes a balance between quick response and moderate overshoot, suiting systems needing both speed and precision. In contrast, Ctrl 2 and Ctrl 3 exhibit longer settling times and higher errors, making them less effective for precise tasks. These results emphasize the effectiveness of LQR-based PID parameters selection to meet specific control objectives compared to the ZN tuning method. For future work, experimental validation on a physical DC motor system is recommended to validate the simulation results. Additionally, investigating these controllers under disturbances and model uncertainties could enhance their robustness for real-world practical applications.

Acknowledgments

The authors acknowledge the financial support of Swiss German University through internal research funds program.

REFERENCES

- [1] D. Mohanraj, J. Gopalakrishnan, B. Chokkalingam, and L. Mihet-Popa, "Critical Aspects of Electric Motor Drive Controllers and Mitigation of Torque Ripple—Review," *IEEE Access*, vol. 10, pp. 73635–73674, 2022, doi: 10.1109/ACCESS.2022.3187515.
- [2] K. S. Mohammad and A. S. Jaber, "Comparison of electric motors used in electric vehicle propulsion system," *Indonesian Journal of Electrical Engineering and Computer Science*, vol. 27, no. 1, pp. 11–19, July 2022, doi: 10.11591/ijeecs.v27.i1.pp11-19.n
- [3] A. Hughes and B. Drury, *Electric Motors and Drives: Fundamentals, Types and Applications*. Newnes, 2019.

-
- [4] E. Akpama, E. Effiong, and R. Ezenwosu, "Simulink design of a DC motor control for water pump using fuzzy logic," *International Conference on Electrical Power Engineering (ICEPENG 2021)*, 2021, pp. 16–19.
- [5] S. Krishnamoorthy and P. P. K. Panikkar, "A comprehensive review of different electric motors for electric vehicles application," *International Journal of Power Electronics and Drive Systems (IJPEDS)*, vol. 15, no. 1, pp. 74–90, Mar. 2024, doi: 10.11591/ijpeds.v15.i1.pp74-90.
- [6] Y. B. Koca, Y. Aslan and B. Gökçe, "Speed Control Based PID Configuration of a DC Motor for An Unmanned Agricultural Vehicle," *2021 8th International Conference on Electrical and Electronics Engineering (ICEEE)*, Antalya, Turkey, 2021, pp. 117-120, doi: 10.1109/ICEEE52452.2021.9415908.
- [7] Hartono, E. Leksono and E. Joelianto, "Type-2 Fuzzy Sliding Mode Control Design for Self-Balancing Mobile Robot," *2023 6th International Conference on Information and Communications Technology (ICOIACT)*, Yogyakarta, Indonesia, 2023, pp. 494-498, doi: 10.1109/ICOIACT59844.2023.10455780.
- [8] R. P. Borase, D. K. Maghade, S. Y. Sondkar, and A. G. Keskar, "A review of PID control, tuning methods and applications," *International Journal of Dynamics and Control*, vol. 9, no. 3, pp. 818–827, 2021. doi: 10.1007/s40435-020-00665-4.
- [9] A. Mulyadi, M. Amin, and M. Anam, "Control Mass-Spring-Damper Based on Tuning Trade-off PID Controller", *Jurnal Ecotipe*, vol. 10, no. 1, pp. 52-60, Apr. 2023.
- [10] S. Das, A. Chakraborty, J. K. Ray, S. Bhattacharjee, and B. Neogi, "Study on Different Tuning Approach with Incorporation of Simulation Aspect for Z-N (Ziegler-Nichols) Rules," *International Journal of Scientific and Research Publications*, vol. 2, no. 8, pp. 1-5, 2018.
- [11] M. P. Dev, S. Jain, H. Kumar, B. N. Tripathi, and S. A. Khan, "Various Tuning and Optimization Techniques Employed in PID Controller: A Review," *Proceedings of International Conference in Mechanical and Energy Technology*, vol. 174, pp. 797–805, 2020.
- [12] F. Cao, "PID controller optimized by genetic algorithm for direct-drive servo system," *Neural Computing and Applications*, vol. 32, pp. 23–30, 2020.
- [13] A. Ahmadi and R. M. Esfanjani, "Automatic tuning of PID controllers using deep recurrent neural networks with pruning based on tracking error," *Journal of Instrumentation*, vol. 19, no. 02, p. P02028, Feb. 2024.
- [14] A. A. Abdelrauf, M. Abdel-Geliel and E. Zakzouk, "Adaptive PID controller based on model predictive control," *2016 European Control Conference (ECC)*, Aalborg, Denmark, 2016, pp. 746-751, doi: 10.1109/ECC.2016.7810378.
- [15] L. Wang, *PID Control System Design and Automatic Tuning Using MATLAB/Simulink*. Hoboken, NJ, USA: John Wiley & Sons, 2020.
- [16] D. Williamson and J. B. Moore, "Three-Term Controller Parameter Selection Using Suboptimal Regulator Theory," *IEEE Transactions on Automatic Control*, vol. 16, no. 1, pp. 82–83, 1971.
- [17] B. Bilgin, J. Liang, M. V. Terzic, J. Dong, R. Rodriguez, E. Trickett, and A. Emadi, "Modeling and Analysis of Electric Motors: State-of-the-Art Review," *IEEE Transactions on Transportation Electrification*, vol. 5, no. 3, pp. 602-617, Sept. 2019, doi: 10.1109/TTE.2019.2931123.
- [18] K. Ogata, *Modern Control Engineering*, 5th ed. Upper Saddle River, NJ, USA: Pearson, 2010.